Nonlinear Elliptic Partial Difference Equations on Graphs

John M. Neuberger

Abstract

This article initiates the study of *nonlinear* elliptic partial difference equations (PdE) on graphs. We seek solutions $u : V \to \mathbb{R}$ to the semilinear elliptic difference equation $-Lu + f(u) = 0$ on a graph $G = (V, E)$, where L is the (negative) Laplacian on the graph G. We extend techniques used to prove existence theorems and derive numerical algorithms for the partial differential equation (PDE) $\Delta u + f(u) = 0$. In particular, we prove the existence of sign-changing solutions and solutions with symmetry in the superlinear case. Developing variants of the Mountain Pass, Modified Mountain Pass, and Gradient Newton Galerkin algorithms to our discrete nonlinear problems, we compute and describe many solutions. Letting $f = f(\lambda, u)$, we construct bifurcation diagrams and relate the results to the developed theory.

1 Introduction.

This paper introduces *nonlinear partial difference equations* (PdE) on graphs. In particular, we prove existence, nodal structure, and symmetry theorems and develop new algorithms for semilinear elliptic PdE. Our efforts parallel recent advances in the study of related partial differential equations (PDE).

Let $G = (V, E)$ be a simple connected graph, with $m = |V|$ and $n = |E|$ finite. For our numerical experiments, we typically take $f : \mathbb{R} \to \mathbb{R}$ to be defined by $f(s) = s^3 + \lambda s$ where λ is a real parameter, although our theorems are generalized to the much wider class of superlinear nonlinearities considered in [1] and [4]. For this example, the primitive $F : \mathbb{R} \to \mathbb{R}$ is

This work was partially supported by NSF grant DMS-0074326

Keywords: superlinear, sign-changing solution, variational method, graphs, GNGA, mountain pass, bifurcation, symmetry.

AMS Subject Classification: 05C50, 35A05, 35A15, 49M15, 58J55, 58J70, 65K10, 90C47.

$F(s) = \int_0^s f(t)\,dt = \frac{1}{4}s^4 + \frac{1}{2}\lambda s^2$. Arbitrarily, we make a choice of orientation for G in order to define $D \in M_{n\times m}$ so that for an edge $e_k = (v_i, v_j) \in E$ we have $D_{ki} = -1$, $D_{kj} = +1$, and $D_{kp} = 0$ for $p \notin \{i, j\}$. Then independently of any choice of orientation, we define the (negative) *Laplacian* $L : \mathbb{R}^m \to \mathbb{R}^m$ to be the linear map represented by the matrix $L = D^T D \in M_{m\times m}$. Numbering our vertices $V = \{v_1, \cdots, v_m\}$ and taking d_i to be the degree of the i^{th} vertex, we see that $L_{ii} = d_i$, $L_{ij} = -1$ if $(v_i, v_j) \in E$ or $(v_j, v_i) \in E$, and $L_{ik} = 0$ otherwise. Identifying $\mathbb{R}^m$ with the set of real-valued functions with domain V, we use the terms "function" and "vector" interchangeably and seek $u \in \mathbb{R}^m$ satisfying

$$-Lu + f(u) = 0. \tag{1}$$

Our study of the finite dimensional difference equation (1) closely follows the related works concerning the PDE

$$\begin{cases} \Delta u + f(u) = 0 & \text{in } \Omega \\ \frac{\partial u}{\partial \eta} = 0 & \text{in } \partial\Omega, \end{cases} \tag{2}$$

as well as the similar zero-Dirichlet problem. The linear operator L has been the object of intense study and much is known about its spectrum. One of the first articles on the subject and an excellent introduction is [2]. Additional references are [10], where an alternate definition of the Laplacian on graphs results in a bounded spectrum, and [3], whose definition coincides with ours. A thorough review of the subsequent literature together with the new ideas of this paper will undoubtedly lead to many additional noteworthy results. It is well known that there are natural zero-Neumann boundary conditions enforced on solutions to the eigenvalue problem

$$-Lu + \lambda u = 0. \tag{3}$$

These conditions also apply to (1). The eigenvalues $\{\lambda_i\}_{i=1,\ldots m}$ satisfy $\lambda_1 = 0 < \lambda_2 \leq \cdots \leq \lambda_m$; we take $\{\psi_i\}_{i=1,\ldots m}$ to be the corresponding eigenvectors, chosen to be orthonormal with respect to the standard Euclidean norm $||u|| = \sqrt{u \cdot u}$ in $\mathbb{R}^m$. The constant eigenvector with eigenvalue 0 can be taken to be $\psi_1 = (\frac{1}{\sqrt{m}}, \ldots, \frac{1}{\sqrt{m}})$.

In [4], a variant of the Mountain Pass Lemma (MPL) is used to duplicate the one-sign existence results of [1], and then extended to prove the existence of a sign-changing exactly-once solution. We apply those ideas to our elliptic

difference equation. In special cases, we can prove the existence of solutions via more elementary techniques. In particular, we show instances where solutions to the nonlinear problem (1) are also eigenfunctions of the linear problem (3). In [16], we developed an algorithm for finding the low energy solutions of [4] using that article's constructive proofs. The one-sign algorithm (essentially the Mountain Pass Algorithm, MPA) is adapted without difficulty; the sign-changing algorithm (Modified Mountain Pass Algorithm, MMPA) requires a significant modification. This difficulty is paralleled when considering existence proofs of sign-changing solutions to (1). In [14], the Gradient Newton Galerkin Algorithm (GNGA) was developed to investigate (2) using a basis of eigenfunctions of the corresponding (continuous) linear problem to span a finite dimensional subspace. We adapt this algorithm in an obvious way, although for small finite m we will use the entire basis. In the spirit of [8], we use knowledge of the symmetry group of G to modify our existence theorems and numerical algorithms to obtain solutions with symmetry.

Let $J : \mathbb{R}^m \to \mathbb{R}$ be defined by

$$J(u) = \frac{1}{2} Du \cdot Du - \sum_{i=1}^{m} F(u_i) \quad \left(= \frac{1}{2} Du \cdot Du - \frac{1}{4} u^2 \cdot u^2 - \frac{1}{2} \lambda u \cdot u \right), \quad (4)$$

where given a function $s : \mathbb{R} \to \mathbb{R}$ and $u \in \mathbb{R}^m$, we take the composition $s \circ u$ to mean $s(u) = (s(u_1), \ldots, s(u_m))$. It is easy to see that

$$J'(u)(v) = -(-Lu + f(u)) \cdot v \quad \left(= Du \cdot Dv - u^3 \cdot v - \lambda u \cdot v \right), \quad (5)$$

so that critical points of J are solutions to (1). Figure 1 depicts typical profiles of $J(tu)$ and $J'(tu)(tu)$. The parallels to the variational setting for the continuous problem (2) are clear. For example, for the zero-Dirichlet version of (2) and under certain assumptions on a subcritical nonlinearity f (see Section 5), the functional $J : H_0^{1,2}(\Omega) \to \mathbb{R}$ defined by

$$J(u) = \int_\Omega \left\{ \frac{1}{2} |\nabla u|^2 - F(u) \right\} dx$$

is C^2 and has directional derivative

$$J'(u)(v) = \langle \nabla J(u), v \rangle = \int_\Omega \left\{ (\nabla u \cdot \nabla v - f(u)v) \right\} dx, \quad \text{for all } v \in H.$$

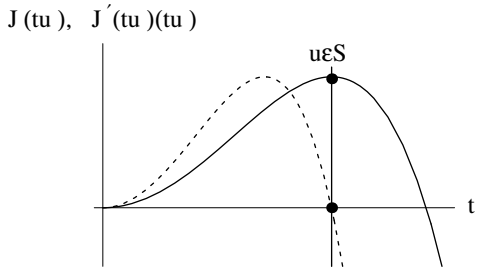

Figure 1: The "Volcano" shape of J drives all superlinear elliptic PDE variational arguments. The same holds for our difference equations on graphs. This diagram is for a random non-zero element of $\mathbb{R}^4$, viewed as a function on the vertices of the complete graph $G = \mathbf{K}_4$, but qualitatively one gets the same picture for other graphs or in the continuous case, for any superlinear f with $f'(0) < \lambda_1$.

In [4] we define the so-called *Nehari manifold*

$$S = \{u \in \mathbb{R}^m - \{0\} : J'(u)(u) = 0\} \tag{6}$$

and an important subset of sign-changing elements

$$S_1 = \{u \in S - \{0\} : J'(u)(u_- - u_+) = 0\}, \tag{7}$$

where $u_+(x) = \max\{u(x), 0\}$ and $u_-(x) = \min\{u(x), 0\}$ for $x \in V$. For the continuous problem, an equivalent definition (and the one found in [4]) is

$$\hat{S}_1 = \{u \in S - \{0\} : u_+ \in S, u_- \in S\}.$$

For our discrete problem, the two definitions of S_1 are *not* equivalent. Indeed, the latter set may be empty or at least fail to have the useful properties exploited in [4]. For both the discrete and continuous problems, $u \in S_1$ implies that

$$J(u)(u_- - u_+) = J'(u)(u_-) - J'(u)(u_+) = 0$$

and

$$J'(u)(u) = J'(u)(u_-) + J'(u)(u_+) = 0,$$

whence $J'(u)(u_-) = J'(u)(u_+) = 0$. For our discrete problem and in light of (18), for $u \in S$ (regardless of whether or not $u \in S_1$),

$$0 = J'(u)(u_\pm) = J'(u_\pm)(u_\pm) + Lu_\pm \cdot u_\mp \geq J'(u_\pm)(u_\pm),$$

whence $J'(u_-)(u_-) = J'(u_+)(u_+)$ yet we do not have $J'(u_-)(u_-) = J'(u_+)(u_+) = 0$. That is, unlike the continuous case, $u \in S_1$ does not imply that $u_\pm \in S$. In any case, we will use (7) in our efforts to find sign-changing solutions to PdE (1). See Section 5 for discussions of the behavior of J acting on or near these sets and the exact hypothesis on f leading to these properties. We will see that S is a manifold (and in fact closed, bounded, and hence compact in this finite dimensional case). In [4], for the superlinear problem and if $f'(0) < \lambda_1$ we have:

Theorem 1.1 *There exist positive and negative solutions to (2) which are local minimizers of $J|_S$, and a sign-changing exactly-once solution that is a minimizer of $J|_{S_1}$.*

In that work and here, nonzero functions have a unique ray projection on to S, i.e., given $u \neq 0$ there exists unique $\alpha > 0$ so that $\alpha u \in S$. For convenience, we refer to this sign-changing exactly-once solution as the CCN solution.

Generalizations of our previous theories and algorithms to non-superlinear problems have been moderately successful (see for example [17], [5], [6], and [7]). One might expect that task to be somewhat easier in the finite dimensional setting of this paper.

Understanding the implications of symmetry is essential in our investigations. In this paper, we demonstrate where such knowledge is useful, leaving deeper graph-theoretic applications and discoveries for subsequent efforts. In particular, consideration of the innovations of [18] and [19] will be of immediate benefit to follow up research done in this new area of nonlinear elliptic PdE on graphs.

The paper is organized as follows. In the next section we state our theorems. In particular, we claim the existence of one-sign and sign-changing exactly-once solutions, along with some solutions of specified symmetry. In Section 3 we provide the basic variational formulations required in the sequel and present the numerical algorithms used in our experimental investigations. These algorithms are variants of the GNGA (see [14], [15], and [19]), the MPA (see [9] and [16]), and the MMPA (see [16], [17], [11], [8]). Many

of these iterative schemes were inspired by constructive proofs, while others provided the insight which lead to new proofs. In Section 4 we analyze several examples of lower order graphs, chiefly the complete graph $\mathbf{K}_3$. In particular, we introduce ideas for investigating the symmetry of solutions. We close the section with some results from new algorithms that will suggest techniques of proof. In Section 5 we provide the proofs for the existence, nodal structure, and symmetry theorems stated in Section 2. Finally, we provide a section containing some concluding remarks and results from considering linear parabolic and hyperbolic PdE.

2 Theorems.

Let f be a superlinear function, not necessarily odd, with $f'(0) < \lambda_1 = 0$ (see Section 5). Then for a connected finite graph G we have:

Theorem 2.1 *There exist positive and negative solutions to (1) which are local minimizers of $J|_S$.*

Theorem 2.2 *There exists a solution to (1) which is a global maximizer of $J|_S$.*

We say a function on G changes sign exactly once if the subgraphs induced by $\{v \in V : u(v) > 0\}$ and $\{v \in V : u(v) < 0\}$ are connected.

Theorem 2.3 *There exists a solution to (1) which changes sign exactly once and is a minimizer of $J|_{S_1}$.*

If $m \geq 3$, we can demonstrate that there exists a solution (distinct from the minimizer) which is a maximizer of $J|_{S_1}$. It seems true that the maximizer of $J|_{S_1}$ and $J|_S$ are one and the same, but we do not have a proof that the maximizer of $J|_S$ is not of one sign.

Let $\mathbf{Q}$ be the symmetry group of G. If f is odd, define $\mathcal{Q} = \mathbf{Q} \times \mathbf{Z}_2$, otherwise take $\mathcal{Q} = \mathbf{Q}$. The possible symmetries of solutions correspond to conjugacy classes of maximal isotropy stabilizer subgroups of $\mathcal{Q}$ (see [19] for more details). Let χ be a fixed point symmetry subspace of $\mathbb{R}^m$ corresponding to a given symmetry, that is, there exists a subgroup in a such a conjugacy class whose elements fix χ pointwise. Then we also have:

Theorem 2.4 *There exists a solution to (1) which is a minimizer of $J|_{S\cap\chi}$. If $\dim(S \cap \chi) \geq 1$, then there exists a second (distinct) solution that is a maximizer of $J|_{S\cap\chi}$.*

It has not been proven that S_1 is a manifold. If it were, and low-dimensional numerical experiments indicate that it can be, the sign-changing proof could be simplified. Never the less, we still have:

Theorem 2.5 *Given a fixed point symmetry subspace χ such that for all $u \in \chi$ with $u_+, u_- \neq 0$ we have $u_+, u_- \in \chi$, there exists a solution to (1) which is a minimizer of $J|_{S_1\cap\chi}$. Given a fixed point subspace χ such that $u \in \chi$ implies $u_+, u_- \neq 0$, there exists a solution to (1) which is a minimizer of $J|_{S\cap\chi}$.*

Apparently, all possible sign-changing solutions with symmetry fall in to one of the two cases. Again, if $\dim(S_1 \cap \chi) \geq 1$, we can demonstrate that there exists a second (distinct) solution that is a maximizer of $J|_{S_1\cap\chi}$. It seems true that the maximizer of $J|_{S_1\cap\chi}$ and $J|_{S\cap\chi}$ are one and the same.

The ability for us to distinguish two solutions as two distinct solutions will depend to some extent on the application. For instance, some solutions will belong to two different fixed point subspaces χ_A and χ_B, whereby it cannot be known without additional information that the same solution u does not satisfy $\min_{S\cap\chi_A} J = \min_{S\cap\chi_B} J = J(u)$. For other fixed point spaces, it will be clear that $\chi_A \cap \chi_B = \{0\} \not\subset S$, so that the corresponding minimizers (and maximizers) will be distinct solutions. In Section 4, we present an example where minimizers and maximizers of $J|_S$, J_{S_1}, $J_{S\cap\chi}$, and $J_{S_1\cap\chi}$ are explicitly and/or numerically found.

3 Variational Structure and Algorithms.

We began our foray in to this new field by extending GNGA to investigate problem (1). For more complicated graphs of higher order, finding the canonical basis of eigenfunctions may entail modification of the ARPACK code found in [18], and definitely will require extending and automating the symmetry analysis and branch following techniques found in [18] and [19].

We assume that $u = \sum_{i=1}^{m} c_i\psi_i$ and seek coefficients $c \in \mathbb{R}^m$ so that the coefficient vector of the standard gradient's eigenfunction expansion $g = (J'(u)(\psi_i))_{i=1,\ldots,m}$ is zero. Note that

$$g_i = Du \cdot D\psi_i - f(u)\cdot\psi_i = (L\sum c_j\psi_j)\cdot\psi_i - f(u)\cdot\psi_i = c_i\lambda_i - f(u)\cdot\psi_i. \quad (8)$$

For small m, the equivalent expression $g_i = Lu \cdot \psi_i - \psi_i \cdot f(u)$ can be computed efficiently without reference to the eigenfunction expansion coefficients c_i. Similarly, the Hessian $h \in M_{m\times m}$ defined by $h = (J''(u)(\psi_i, \psi_j))_{i,j=1,\dots,m}$ can be computed as

$$h_{ij} = D\psi_i \cdot D\psi_j - f'(u)\psi_i \cdot \psi_j = \lambda_i \delta_{ij} - f'(u)\psi_i \cdot \psi_j, \tag{9}$$

where δ_{ij} is the Kronecker delta. Applying Newton's method with stepsize $\delta \in (0, 1]$ to find zeroes of g results in our algorithm:

1. Initialize $c = c^0 \in \mathbb{R}^m$ and set $u = u^0 = \sum c_i \psi_i$.
2. Loop until $||\nabla J(u)|| = \sqrt{g \cdot g}$ is small:
   (a) Compute the gradient vector $g \in \mathbb{R}^m$.
   (b) Compute the Hessian matrix $h \in M_{m\times m}$.
   (c) Solve for the search direction χ satisfying $h\chi = g$.
   (d) Step $c = c^{k+1} = c^k - \delta\chi$.
   (e) Update $u = u^{k+1} = \sum c_i \psi_i$.
   (f) Output data, compute norm of gradient.

The output data can vary depending on the experiment; typical choices include the value of $J(u^k)$, calculated similarly to the gradient and Hessian, and the signature $\mathrm{sig}(u^k)$, which we take to be the number of negative eigenvalues of $h = h(u^k)$. If u is a nondegenerate solution to (1), then $\mathrm{sig}(u)$ equals the Morse index (MI) of u. The MI can be thought of as the number of "down" directions of the critical point, e.g., MI $= 0$ for minima, MI $= m$ for maxima, and MI$\in \{1, \dots, m-1\}$ for saddle points in between. The search direction χ can be solved using any number of linear solvers, even dealing with possibly noninvertible Hessians h. Noninvertible Hessians inevitably occur at boundaries of basins of attraction of Newton's method, fractal when taking discrete steps, and at degenerate critical points. This is good news actually, since the first situation can be avoided by knowing good guesses and the second can lead to interesting symmetry-breaking bifurcations.

We also present a few experimental results relating to adaptations of the MPA and MMPA from [16]. In part, we do so because their operation exposes the existence theory. In [4] and [16], we see that given $u \neq 0$ there exists $\alpha > 0$ such that $\alpha u \in S$. This holds true for our current (discrete) problem

as well. In [4] and [16], one sees that S_1 has the property that given a sign-changing function u there exist $\alpha, \beta > 0$ so that $\alpha u_+ \in S$, $\beta u_- \in S$, and as a result, $\alpha u_+ + \beta u_- \in S_1$. For our current (discrete) problem, we will see that given a sign-changing function u there exists $\alpha > 0$ and $t \in (0, 1)$ so that, with z defined by $z = \alpha((1-t)u_+ + tu_-)$, we have $J'(z)(z_- - z_+) = 0$ and hence $z \in S_1$. Combining these constraints with Sobolev gradient steepest descent (see also [20]) results in the MPA for finding MI 1 one-sign solutions and the MMPA for finding MI 2 sign-changing solutions of (2). The brief pseudocode is as follows:

1. Choose $u = u_0$ as a one-sign element of function space.
2. Project u on to S by doing steepest ascent in the ray direction.
3. Compute approximation of $\nabla J(u)$ by solving appropriate linear system.
4. Loop until approximation of $\nabla J(u)$ is small:
   (a) Take gradient descent step: $u_{k+1} = u_k - \delta \nabla J(u_k)$.
   (b) Project u on to S by doing steepest ascent in the ray direction.
   (c) Compute approximation of $\nabla J(u)$ by solving linear system.

Here, $\delta \in (0, 1]$ is the stepsize, and the linear system in question (for the continuous zero-Dirichlet problem (2)) satisfies $-\Delta(\nabla J(u)) = \nabla_2 J(u)$ where $\nabla_2 J(u)$ is the "usual" Euclidean gradient. Borrowing from the method used in [11], we can construct a Sobolev gradient for our discrete Neumann problem that has the good performance indicative of using the proper norm (see Figure 5). Defining g_i as in (8), we obtain the Sobolev gradient

$$\nabla_S J(u) = g_1 \psi_1 + \sum_{i=2}^{m} \frac{g_i}{\lambda_i} \psi_i.$$

The MMPA requires one to start with a sign-changing initial guess and to project iterates on to S_1 as opposed to S. For the continuous problem, this can be accomplished by

$$P_{S_1}(u) = \alpha u_+ + \beta u_-,$$

where $\alpha, \beta \in (0, \infty)$ are chosen so that $\alpha u_+ = P_S(u_+)$ and $\beta u_- = P_S(u_-)$ are on S. Projecting functions on to S is just steepest ascent in the ray direction

(see Figure 1 and Section 5). Briefly, starting with $u_0 = u$ and iterating

$$u_{k+1} = u_k + \delta \frac{J'(u_k)(u_k)}{|u_k|^2} u_k$$

results in convergence to $P_S(u)$. The term $J'(u_k)(u_k)$ can be approximated in several ways of varying degrees of numerical complexity, efficiency, and accuracy, including using the eigenfunction expansion ideas from [11]. For our discrete problems, the projections of iterates on to S_1 must be accomplished via a different method. We will see in Section 5 that given a sign-changing vector $u \in \mathbb{R}^m$, the path

$$z(t) = P_S(r(t)) = P_S((1-t)u_+ + tu_-) = \alpha(t)((1-t)u_+ + tu_-)$$

has essentially the same properties as it did in the continuous case. We will show that

$$\begin{aligned} \tfrac{d}{dt}J(z) &= J'(z)(\alpha' r + \alpha r') \\ &= \tfrac{\alpha'}{\alpha} J'(z)(z) + \alpha J'(z)(u_- - u_+) = \alpha J'(z)(u_- - u_+) \end{aligned} \tag{10}$$

is zero only for some unique $t^* \in (0,1)$ so that $J(z(t^*)) > J(z(t))$ for all $t \in [0,1] - \{t^*\}$, and that in fact $z(t^*) \in S_1$ as defined in (7) (see Figure 6). If $u \in S_1$, then $t^* = \frac{1}{2}$ and $\alpha(t^*) = 2$. Thus, given a sign-changing vector u we take gradient ascent steps in the $u_- - u_+$ direction and project iterates on to S, until the maximum value is achieved and we are on S_1. For example, the *Mathematica* fragment for effecting these projections (efficient enough for small problems) which uses the built in secant method is:

```
up[u_] := Table[If[u[[i]] > 0, u[[i]], 0], {i, 1, m}];
um[u_] := -up[-u];

PS[u_] := u * FindRoot[t (L.u).u - u.f[t u] == 0, {t, .5, 3.5},
              MaxIterations -> 100][[1, 2]];

z[t_, u1_, u2_] := PS[(1 - t)u1 + t u2];
alph[u1_, u2_]  :=
   FindRoot[(u2 - u1).(L.z[t, u1, u2] - f[z[t, u1, u2]]) == 0,
      {t, .3, .7}, MaxIterations -> 100][[1, 2]];
PS1[u_] := z[alph[u1,u2], u1, u2];
```

We will employ algorithms which are further variants of the MPA and MMPA. First, since we are in a finite dimensional setting, we can do steepest ascent and find critical points (solutions to (1)) which are maximizers. This is easily accomplished by replacing

$$u_{k+1} = u_k - \delta \nabla J(u_k)$$

with

$$u_{k+1} = u_k + \delta \nabla J(u_k).$$

Secondly, we borrow from ideas in [8] and [19] and restrict our optimization to invariant subspaces corresponding to specified symmetries. For example, when seeking a solution vector in $\mathbb{R}^3$ when G is the complete graph $\mathbf{K}_3$, we might want to restrict our search to elements of the form (b, b, a) in an invariant subspace χ_B (see the $\mathbf{K}_3$ example in Section 4). Given a vector $u = (b_1, b_2, a)$, we execute the projection

$$P_{\chi_B}(u) = \left(\frac{b_1 + b_2}{2}, \frac{b_1 + b_2}{2}, a \right) \tag{11}$$

after each gradient step. In theory, the gradient $\nabla J(u)$ is invariant under the group actions corresponding to the chosen symmetry, but in practice, small computational errors will lead to instability. The projection $u_k = P_S P_{\chi_B} \hat{u}_k$, for example, will ensure that the iterate u_k is an element of the manifold which maintains the symmetry of type B. Other symmetry types corresponding to other subgroups can be similarly enforced.

4 Examples.

In this section we demonstrate the numerical and analytical techniques by looking at a relatively simple example, namely the complete graph $\mathbf{K}_3$. We are able to prove some extra facts in this concrete case, but more importantly we show the inner workings of each algorithm and theorem. We take a thorough approach in looking at this problem, with an eye towards testing our new algorithms and gaining insight in to the structure needed to prove existence and nodal structure theorems.

Our initial experiments on regular square grids were entirely analogous to those found in [14]. Differing in scale via factors of the mesh-size Δx missing in the differentiation and integration, one immediately realizes that

the programs are virtually identical. We do not find it worthwhile to report here further on these executions other than to note that it is enlightening to be reminded that using numerical algorithms to solve PDE are really attempts to solve discrete problems exactly.

In this paper, our goal is to introduce nonlinear elliptic PdE on graphs and techniques for investigating them. By understanding the underlying symmetries of a given graph G, one should be able to choose a useful order for the basis of eigenfunctions of L for $\mathbb{R}^m$. This is an essential step for understanding the expected proliferation of symmetric solutions, aiding in both our numerical investigations and subsequent efforts to find existence and nodal structure proofs. Adapting the ARPACK code (see [18]) and automated branch following methods (see [19]) that we have so successfully used on continuous problems, we will then be able to thoroughly investigate very large graphs with large numbers of symmetries. Applying the sophisticated approach taken in [18] and [19] (where the $\mathbf{D}_6 \times \mathbf{Z}_2$ symmetry of the hexagon (Koch's Snowflake) is exploited) will be a fruitful area for several reasons. Applying those concepts, the symmetry of the graph (and hence the basis) can be used by an automated program which follows the trivial branch, makes a turn at each eigenvalue (bifurcation point), and continues making turns at each secondary (or tertiary) bifurcation point. At each turn this automated code uses the critical eigenfunctions of the Hessian to perturb off of the parent branch. This approach is particularly interesting at multiple critical eigenvalues, where algorithmic knowledge of the symmetry of the basis (and hence possible symmetries of solutions) is required in order to follow all possible types of (conjugacy classes of) branches. This is achieved via applying knowledge of the structure of the symmetry group of the graph G. The future development of the new field of nonlinear elliptic PdE on graphs will rely heavily on the ideas in [18] and [19], where in theory a single push of a button may almost completely generate an accurate and informative bifurcation diagram annotated with a plethora of relevant information concerning existence, multiplicity, symmetry, nodal structure, MI, and so on. The present paper is just the opening round.

4.1 $\mathbf{K}_3$.

Our main example demonstrates that for simple graphs one can work out the existence and "nodal structure" of some solutions exactly, while unexpected complexities result in a structure rich enough to provide secondary bifur-

cations and solutions not easily come by analytically. Let $G = \mathbf{K}_3$ be the complete graph with 3 degree-2 vertices. There is in some sense a maximal amount of symmetry to exploit in complete graphs.

Due to the superlinear nature of the nonlinearity f, the graph of J for $\lambda < \lambda_1 = 0$ is a "volcano", e.g., 0 is a local minimum, each ray intersects the rim (the manifold S) once, and so on. Indeed, these properties drive all of the existence proofs in [4] and many related works. Figure 1 shows the graphs of $J(tu)$ and $J'(tu)(tu)$ for a randomly selected nonzero vector in $\mathbb{R}^4$ (function on the vertices of $G = \mathbf{K}_4$), but one gets qualitatively the same diagram in the present $\mathbf{K}_3$ case.

In initial experiments, we used the basis of eigenfunctions of L for $\mathbb{R}^3$ that was automatically provided by *Mathematica*. Subsequently, we found the basis (13) to be a more convenient choice. It demonstrates eigenfunctions of each symmetry type, although this was not quite the case for $\mathbf{K}_4$. The matter of choosing a proper basis in general has not quite been settled. Plugging $u = c\psi_i$ in to (1), one easily obtains complete information about several branches. The trivial branch is $c \equiv 0$. Along the one-sign branch $u \equiv c$ bifurcating to the left from $\lambda_1 = 0$, one has $c^2 = -\lambda$ and $J(cu) = \lambda^2$. The conjugacy class of the permutations of $u = c(-1, 1, 0)$ has branches bifurcating to the left from $\lambda_2 = \lambda_3 = 3$, where $c^2 = 3 - \lambda$ and $J(cu) = \frac{1}{2}(3-\lambda)^2$. For $G = \mathbf{K}_4$, another special case was the class represented by $u = c(-1, -1, 1, 1)$, where also $c^2 = 4 - \lambda$ but $J(cu) = (4 - \lambda)^2$. It is not so easy to work out in closed form the results for solutions which are not exact multiples of eigenfunctions. For example, there are solutions which asymptotically approach small multiples of (permutations of) the eigenfunction $(2, -1, -1)$ as they bifurcate from the multiple eigenvalue. In this supposedly simple example, there are secondary bifurcations. Note that the secondary bifurcation point on the one-sign branch can be found exactly for any complete graph (see (14)). These secondary solutions are not multiples of an eigenfunction; it would be difficult if not impossible to determine its character without using an algorithm such as GNGA, which we used in all initial $\mathbf{K}_4$ and $\mathbf{K}_3$ experiments, or one the modified MPA-type algorithms.

To demonstrate the symmetry arguments from [18] and [19] to which we have alluded, we more carefully analyzed the symmetry of eigenfunctions and solutions. The symmetry group for G is $\mathbf{D}_3$, that is, 6 rotations and rotations. Allowing for sign changing anti-reflections, our group expands to $\mathbf{D}_3 \times \mathbf{Z}_2 \simeq \mathbf{D}_6$. Forming the 16 subgroups of $\mathbf{D}_6$ and translating back to $\mathbf{D}_3 \times \mathbf{Z}_2$, we see that there are 5 symmetry types of solutions. These are

# Classes	Symm. Type	Elements	Dim Invar. Subspace
1	A	(a,b,c)	$\dim(\chi_A \cap S) = 2$
3	B	(b,b,a) (a,b,b) (b,a,b)	$\dim(\chi_{B_i} \cap S) = 1$ i=1,2,3
1	C	(a,a,a)	$\dim(\chi_C \cap S) = 0$
3	D	(-b,b,0) (0,-b,b) (b,0,-b)	$\dim(\chi_{D_i} \cap S) = 0$ i=1,2,3
1	E	(0,0,0)	$\chi_E \cap S = \emptyset$

Table 1: For $\mathbf{K}_3$, the manifold S is 2 dimensional. The intersection of the invariant subspaces with S is of one lower dimension than the invariant subspaces themselves. All solutions belong to one or more of the appropriate intersections. From the ordering in (12), we see that $\chi_E \subset \chi_C \subset \chi_{B_i} \subset \chi_A$ and $\chi_E \subset \chi_{D_i} \subset \chi_A$.

the 5 conjugacy classes of maximal stabilizer (isotropy) subgroups. The fact that the number of symmetry types for $\mathbf{K}_3$ is smaller than for $\mathbf{K}_4$ explains why we have chosen this example for our discussion on the implications of symmetry.

A representative of a symmetry class corresponds to a subspace which is invariant under the actions of that subgroup. The symmetry types can be partially ordered as

$$A \prec B \prec C \prec E \text{ and } A \prec D \prec E \tag{12}$$

where, for example, $B \prec C$ means that if $H \in B$ and $K \in C$ then H is a subgroup of K. See Table 4.1 for a summary of the invariant subspaces corresponding to these 5 symmetry types. A is the symmetry which corresponds to the subgroup containing only the identity. Solutions of this type have no symmetry. B is the symmetry type of the flip, i.e., each element of the class fixes a function of the form (b, a, b) (or one of its permutations) on $G = \mathbf{K}_3$. Symmetry type C fixes only the constant functions, i.e., invariance under both rotations and flips. Symmetry type E corresponds to the whole symmetry group and fixes only the trivial solution $u = 0 \in \mathbb{R}^m$. Finally, symmetry type D corresponds to invariance under anti-flips, e.g.,

functions of the form $(b, 0, -b)$ (or one of its permutations) on $G = \mathbf{K}_3$. A natural goal for future efforts will be to systematize and automate the construction of the hierarchy (lattice) of symmetry types for each new graph investigated. In Figure 3, the primary branch of constant solutions (multiples of ψ_1) is of symmetry type C, invariant under all rotations and flips. The only subgroups of the subgroup of type C are of symmetry types B and A, which have invariance under flips, and only the identity, respectively. Thus, the only possible bifurcations at $\lambda = -\frac{3}{2}$ off of the constant branch are of symmetry types B and A. The displayed secondary branch is of symmetry type B, with eigenvector expansion coefficients of the form $(c_1, 0, c_3)$, indicating that added to the type C ψ_1-component is some amount of the type B ψ_3-component $((1/\sqrt{6})(-1, -1, 2))$. The lower portion of the secondary branch (which could be viewed as a separate branch) was found in $\mathbf{K}_4$ experiments as well. Armed with this symmetry information, the somewhat trial and error process suggested by Figure 4 is perhaps unnecessary although still informative. For example, without using the deeper implications of the Equivariant Branching Lemma (see [12]) and considering higher order derivatives of J, we cannot be certain that we have not missed an asymmetric branch (type A) bifurcating from the constant solution branch at this location. Since the extrema in Figure 4 are all of symmetry type C, we can be fairly confident however. The following experiments using Sobolev gradient descent and ascent restricted to invariant subspaces (see also Figure 2) gives further evidence that there is no such missing branch.

We have found 3 different types of solutions of symmetry type B at $\lambda = -4$. There are a total of 18, since each type has 3 rotations (the type B conjugacy class has 3 subgroup elements) and the negative of each solution is a solution. Let χ_B be an invariant subspace corresponding to one of these conjugacy classes, say the one with elements of the form (b, b, a). Intersecting this 2-dimensional subspace with the Nehari manifold S results in a 1-dimensional sub manifold containing all symmetry type B solutions from this conjugacy class. Minimizers and maximizers of J restricted to this sub manifold must be solutions of symmetry type B or C, since $B \prec C$ implies that $\chi_C \subset \chi_B$ and the trivial type E solution is not an element of S. Let $q(\theta) = P_S(\cos(\theta), \cos(\theta), \sin(\theta))$. Then the range of q is precisely the 1-dimensional manifold $\chi_B \cap S$. Figure 2 shows the graph of $J \circ q$, with 4 of the 8 extremal points and their corresponding MI noted. These points are solutions to (1) which have either symmetry type B, or in the case of the constant solutions, symmetry type C. The solutions are also noted on

the portion of the bifurcation diagram found in Figure 3. It is interesting to note that minimizers in this invariant subspace can be of either MI 1 or MI 2; all we know is that there is at least one more "down direction" by virtue of being an element of S.

The modifications of the MPA and MMPA obtained by restricting to invariant subspaces work well (keep in mind $f'(0) = \lambda < \lambda_1 = 0$ must be assumed for S to be a manifold). In many low-dimensional cases, the invariant subspace has a 0 or 1 dimensional intersection with S or S_1. The former leads to a solution in 1 iteration, while the latter efficiently leads to convergence by performing what amounts to 1-dimensional steepest descent and/or ascent. The 4 featured solutions noted in Figures 2 and 3 were all separately (and efficiently) located using the MPA modified to perform steepest descent and/or ascent in χ_B (see (11), $B = B_1$ corresponds to the conjugacy class with symmetry (b, b, a)). Such results are easily verified, since plugging a solution vector in to (1) is a simple matter. Although we have not proven that S_1 is a manifold, it appears from our experiments that it is when $G = \mathbf{K}_3$. If so, clearly it is of dimension 1. We can see that $\chi_B \cap S_1$ is not empty, since letting $u = (-1, -1, 2)$ we have $u, u_+, u_- \in \chi_B$ hence $z(t) = P_S((1-t)u_+ + tu_-) \in \chi_B \cap S_1$ for all $t \in [0, 1]$. Thus, $\chi_B \cap S_1$ is zero dimensional, in fact containing precisely two points, the solution $z(t^*) \in S_1$ obtained by maximizing $J \circ z$ on $[0, 1]$, and the "antipodal" solution gained by replacing u with $-u$, $(1, 1, -2)$.

For good measure, GNGA was also employed to verify the results of executing the symmetry invariant versions of the MPA and MMPA.

We looked for but did not find a solution of symmetry type A. Without deeper theory, one might expect branches of this type to bifurcate from just about anywhere, as $\chi \subset \chi_E$ for all other fixed point subspaces χ. In particular, we looked along the symmetry type B branch since only the subgroup corresponding to symmetry type A is a subgroup of type B subgroups. At this time we cannot know one way or the other if secondary bifurcation of this type ocurrs for large negative values of λ; no $\mathbf{K}_3$ or $\mathbf{K}_4$ experiments yielded non-symmetric solutions.

We will see in Section 5 that much of what we have observed can be proved. In particular, we can prove that solutions of each symmetry type must exist, up to inclusion. For example, in our $\mathbf{K}_3$ experiment we found solutions of types B, C, D, and E. The "missing" type-A solutions were never guaranteed, as every solution belongs to the fixed point subspace having no symmetry (namely, $\mathbb{R}^m$).

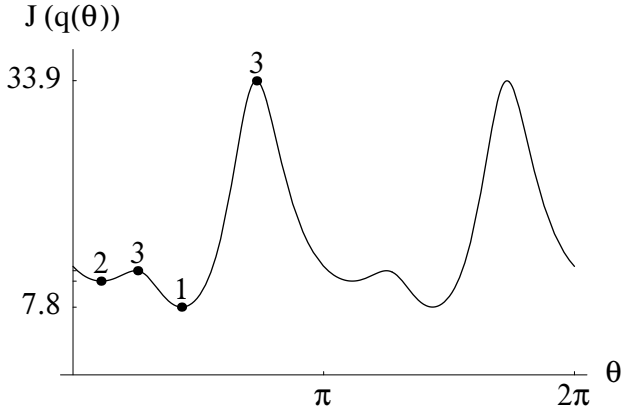

Figure 2: Graph of the functional J restricted to the 1-dimensional set obtained by intersecting a type-B invariant subspace for $\mathbf{K}_3$ with the manifold S. Extremal points are solutions. See Figure 3 to view the locations of these solution on the bifurcation diagram depicting all symmetry type B solutions.

4.2 MPA and MMPA.

In preparation for looking for existence proofs of the type found in [4], we looked for low-energy solutions using the MPA and a modified version of the MMPA. The above $\mathbf{K}_3$ symmetry type B experiments used the MPA, modified as noted in Section 3, equation (11). The Sobolev gradient can be easily computed as in [11] by dividing the eigenfunction expansion coefficients of the gradient by the eigenvalues:

$$\nabla_S J(u) = g_1\psi_1 + \sum_{i=2}^{m}(g_i/\lambda_i)\psi_i,$$

where the coefficients $g_i = J'(u)(\psi_i)$ are exactly as in the GNGA. Using a purposefully bad initial guess at $\lambda = -.5$, namely $u_0 = (-1, 0, 1, 1)$, the MPA converged to the one-sign (constant) solution $(\frac{\sqrt{2}}{2}, \frac{\sqrt{2}}{2}, \frac{\sqrt{2}}{2}, \frac{\sqrt{2}}{2})$ in 7 iterations. Convergence in "7 iterations" is something of a meta-theorem, generally implying that an appropriate space, norm, and hence gradient were used. The plot on the left in Figure 5 depicts the norm of the gradient as a function of MPA iteration number for this particular execution.

We indicated in Section 3 that we must use the alternate definition of S_1 found in (7). The difficulty is quite interesting. In [4], and as a result

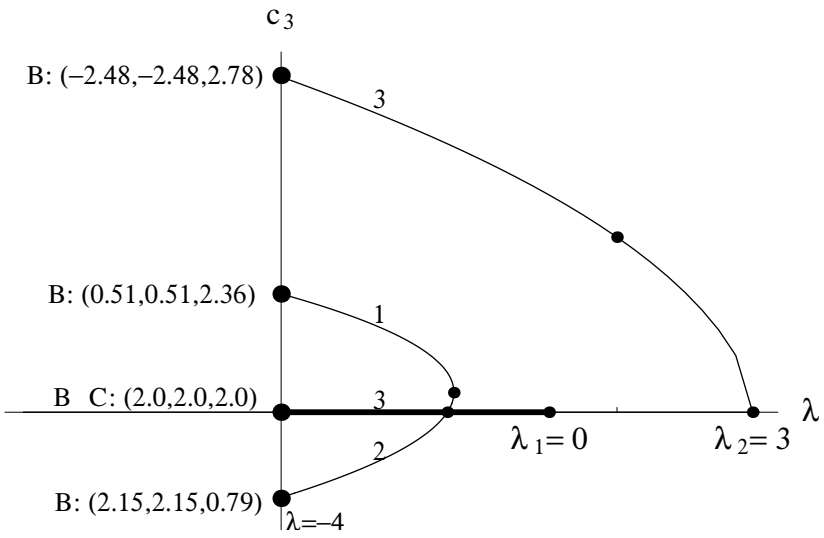

Figure 3: All symmetry type B solutions to (1) when $G = \mathbf{K}_3$ can be found in this diagram. Each non constant branch corresponds to 6 solutions, plus-or-minus from each of the 3 conjugacy classes. The small dots indicate bifurcation points where the Hessian is singular. The 4 large dots denote solutions located on the graph in Figure 2; approximate values of the solutions at $\lambda = -4$ are given. The thick line on the λ axis is the constant solution bifurcating to the left from $\lambda = 0$. The λ axis also corresponds to the trivial type E solution, although this is not an element of $\chi_B \cap S$ since $0 \notin S$. The eigenvector expansion coefficients are of the form $(c_1, 0, c_3)$, indicating that added to the type C ψ_1-component is some amount of the type B ψ_3-component.

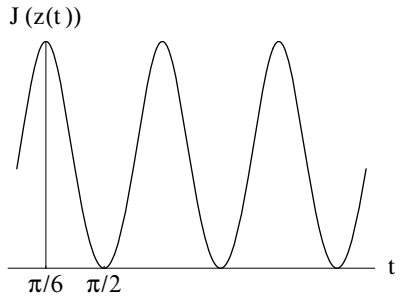

Figure 4: A method for finding perturbation directions at a bifurcation point. Here, $z(t) = \alpha(t)(u^* + \cos(t)\psi_2 + \sin(t)\psi_3)$, where u^* is the one-sign solution (multiple of constant eigenfunction ψ_1) at $\lambda^* = -\frac{3}{2}$, $\lambda = -\frac{7}{4}$ is just to the left of the bifurcation point, and $\alpha = \alpha(t)$ is chosen so that $z \in S$ for all $t \in (0, 2\pi)$. The 3 minima correspond to points that are reasonably likely to be in the basin of attraction of MI 1 solutions, while the maxima should lead towards MI 2 solutions. That ψ_2 and ψ_3 span the critical eigenspace follows from (14) in the $\mathbf{K}_3$ case presented here. The realization of α is the steepest ascent in the ray direction portion of the MPA algorithm. It may be necessary to take small stepsizes approximating continuous Newton's method in order to prevent unintended iterations resulting from the discrete algorithm's fractal basin of attraction boundaries. Due to the fact that in hindsight the MI 2 $\rightarrow$ MI 1 branch depicted on the left in Figure 3 initially bifurcated to the right, we could have presented this plot at (say) $\lambda = -1.49$, whence a somewhat different profile would be apparent. For brevity, we do not include the other secondary branches which were obtained in this fashion. This method can be effective, but still requires a certain amount of trial and error and is no substitution for the techniques in [19] where symmetry is exploited instead.

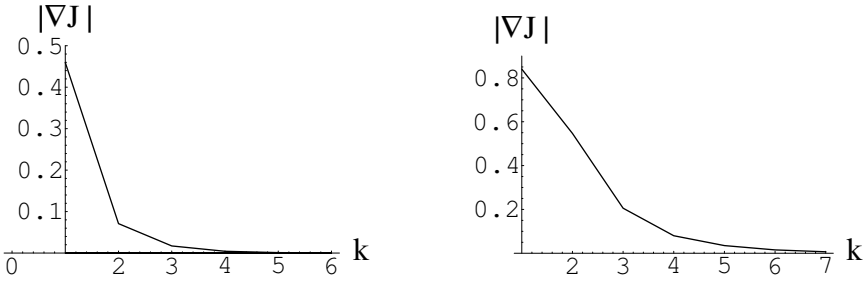

Figure 5: Convergence of MPA to the constant one-sign and the modified MMPA to the sign-changing exactly-once solutions of (1) for $G = \mathbf{K}_4$ at $\lambda = -\frac{1}{2}$. Despite starting with intentionally bad initial guesses, both algorithms yield solutions accurate to 4 or 5 decimal places in $k = 7$ iterations, with $|\nabla_S J(u_7)| = \sqrt{g_S \cdot g_S} \approx 10^{-4}$.

in [16], we rely heavily on the fact that since u_+ and u_- are disjoint, then $J(u) = J(u_+) + J(u_-)$. It also follows that $J'(u)(u_+) = J'(u_+)(u_+)$, so that $u_+, u_- \in S$ implies that u_{S_1}. None of these statements is true for graphs. Intuitively, the problem lies in the fact that positive and negative vertices are not necessarily separated by zero vertices. Thus, in general $Lu_+ \cdot u_- \neq 0$. We were able to do quite a bit of analysis in the form of minor lemmas by first showing that $Lu_+ \cdot u_- \geq 0$ (see (18)). This fact follows from noticing that the only nonzero terms are obtained by subtracting the negative neighbors from positive boundary terms. Our alternate definition for S_1 makes the MMPA work, and once we have proven that the new set has many of the same properties as found in [4] (see Section 5), we will be able to prove the existence of a sign-changing exactly-once solution. Figure 6 suggests that, like the explicit construction in [4], along the convex combination projected on to S connecting positive and negative parts of a sign-changing function u, J achieves its maximum at or near the midpoint. We will see that every path on S connecting a positive function to a negative function will intersect S_1. This separation property will be the key ingredient in our sign-changing existence proof and demonstrates why the CCN solution should be of MI 2 (the second concave down direction is always the ray direction for any element of S).

Using the same initial guess as in the MPA example resulted in (by virtue of symmetry invariance and pure dumb luck) pseudo convergence of the

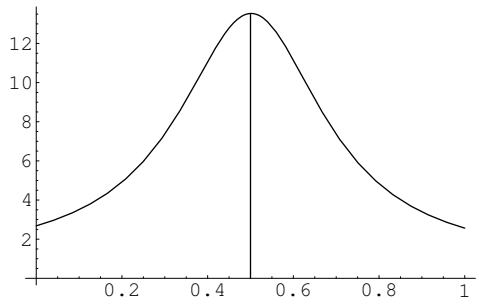

Figure 6: This plot of $J(z(t)) = J(P_S(r(t))) = J(P_S((1-t)u_+ + u_-))$ could have easily come from a continuous problem, although it was in fact generated using a specific sign-changing vector $u \in \mathbf{R}^4$ while studying $G = \mathbf{K}_4$. In this example, u satisfied $u, cu_+, cu_- \in S$ for some $c \in (0,1)$, which we originally thought might be a suitable definition for S_1 (in the continuous case this works if we insist that $c = 1$). Noticing that the maximum occurred close to but not exactly at $t = \frac{1}{2}$ lead to the alternate definition (7). If $u \in S_1$, then the maximizer would occur at precisely $t = \frac{1}{2}$.

MMPA to a MI 3 solution in just a few iterations. Allowing the algorithm to execute for another 100 iterations, one sees that 2 constraints are not enough to find a MI 3 solution which could be viewed as a MI 1 saddle point of $J|_{S_1}$; the algorithm proceeded to converge to the proper CCN MI 2 minimal energy sign-changing exactly-once solution. The plot on the right in Figure 5 is the result from using the initial guess from Figure 6, where once again we observed the "7 iteration convergence" to a solution accurate to roughly 5 decimal places. In fact, it was a known exact solution obtained in the $\mathbf{K}_4$ experiments when $\lambda = -\frac{1}{2}$.

4.3 Other Graphs and General Results.

We considered other graphs, although we do not plan to report much of the findings in this paper. In fact, our first GNGA experiments were on the circulant graph $G = \mathbf{C}_{13}(1,3,4)$ which has $m = 13$ vertices and $n = 39$ edges. The eigenvalues of L are approximately

$$\sigma = \{0, 4.69722, \ldots, 4.69722, 8.30278, \ldots, 8.30278\},$$

with 2 multiplicity 6 eigenvalues. These values can be in theory calculated using algebraic equations. We computed the various symmetry types of eigenfunctions (vectors in $\mathbb{R}^m$), 6 for each of the two distinct multiple eigenvalues. See Figure 7 for a plot of a solution to (1) for $\mathbf{C}_{13}(1,3,4)$. We are not including the rest our experimental bifurcation results for this graph, deferring such reporting until the advances found in [18] and [19] have been incorporated. The next experiment we did was on $\mathbf{K}_4$, where we used elementary techqniques, GNGA, and a certain amount of trial and error. We did eventually obtain complete results paralleling the $\mathbf{K}_3$ results presented above, but we are again not reporting the details here. The simple experiments done on $\mathbf{K}_3$ and the resulting complexities should be enough to convince the reader that when considering a general graph G, it will be necessary to first thoroughly understand the implications of the graph's symmetries, order a basis, and automate the branch following code.

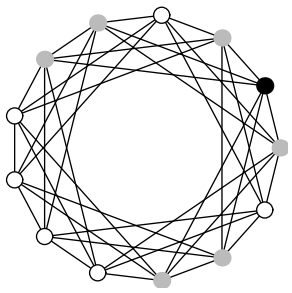

Figure 7: A "contour plot" of a MI 6 sign-changing solution to (1) for $G = \mathbf{C}_{13}(1,3,4)$. We used an arbitrary sign-changing initial guess projected onto S at $\lambda = 4 < \lambda_2 \approx 4.69722$. Here, black corresponds to a large positive value, gray to small absolute values, and white to large negative values. The resulting solution is sign-changing "exactly-once" (although not the minimal energy MI 2 CCN solution) in the sense that the positive and negative vertices form connected subgraphs.

We now contemplate what can be said in general about nonlinear elliptic difference equations on complete graphs. It is not difficult to see that the complete graph $\mathbf{K}_m$ has a simply described set of eigenvectors. It can be easily verified that the rows of the following matrix are an orthogonal basis for $\mathbb{R}^m$, with the first row being an eigenvector corresponding to zero, and

the last $m-1$ rows being eigenvectors corresponding to the multiplicity $m-1$ eigenvalue $\lambda_2 = \lambda_3 = \cdots = \lambda_m = m$.

$$\Psi = \begin{bmatrix} 1 & 1 & 1 & 1 & 1 & \cdots & 1 \\ -1 & 1 & 0 & 0 & 0 & \cdots & 0 \\ -1 & -1 & 2 & 0 & 0 & \cdots & 0 \\ -1 & -1 & -1 & 3 & 0 & \cdots & 0 \\ \cdot & \cdot & \cdot & \cdot & \cdot & \cdots & \cdot \\ -1 & -1 & -1 & -1 & -1 & \cdots & 0 \\ -1 & -1 & -1 & -1 & -1 & \cdots & m \end{bmatrix}. \tag{13}$$

It may be that the above basis is still not in "canonical form", i.e., is not projected in such a way as to decompose function space in to the possible types of symmetry. It appears, however, to do so for the 3×3 $\mathbf{K}_3$ case. Without applying the theory of symmetry groups to this end, there is a certain amount of trial and error in constructing the bifurcation diagram associated with (1). On the one hand, $\mathbf{K}_m$ is fairly simple and well studied; on the other, it has a large symmetry group. For our purposes, the above basis suffices for several demonstrations. As we first saw when analyzing the $\mathbf{K}_4$ problem, we can show that there exists and describe completely the constant branch bifurcating from $\lambda_1 = 0$ and do the same for the conjugacy class of permutations of Ψ_2 (since it has only ± 1 and 0 entries). Adding even rotations of Ψ_2 to each other results in another eigenvector with only ± 1 and 0 entries, whereby the same type of calculations apply. In these cases, solutions of the nonlinear problem are multiples of eigenfunctions. We were unable to find an easy way to prove the existence of the other branches in a similarly elementary fashion when solutions do not correspond exactly to multiples of eigenfunctions, although the GNGA can certainly find them. Further, when G is a complete graph a straightforward calculations shows that at $\lambda = -\frac{m}{2}$ the Hessian matrix is

$$h = \begin{bmatrix} -m & 0 & 0 & \cdots & 0 \\ 0 & 0 & 0 & \cdots & 0 \\ \cdot & \cdot & \cdot & \cdots & \cdot \\ 0 & 0 & 0 & \cdots & 0 \\ 0 & 0 & 0 & \cdots & 0 \end{bmatrix}. \tag{14}$$

Thus, it is proven that there is a multiplicity $m-1$ zero eigenvalue and hence a bifurcation point with a jump from MI 1 to MI m at $\lambda = -\frac{m}{2}$ as one travels left along the constant branch starting from $\lambda_1 = 0$.

This concludes our numerical experiments and musings concerning what could be proven for the explicit case when G is a complete graph. In the next section, we will prove the existence of one-sign and sign-changing solutions, in general and of specified symmetry. The proofs are inspired by the work in [4], but many of the required techniques only came to light after the variants of the MPA and MMPA were correctly stated, coded, and tested. In particular, the correct definition of S_1 found in (7) was discovered during the consideration of certain experimental failures. We first coded the MMPA attempting to use the old method $v = P_{S_1}u = P_S(P_S u_+ P_S u_-)$, but found that $v_+, v_- \notin S$. Following paths as in Figure 6 lead to the realization that it was maximizers of such paths that was going to play the desired separation role, despite the fact that no longer could we expect $u \in S_1$ to imply that $u_+, u_- \in S$. As a final note on our numerical experiments, we tested the MMPA (and other algorithms) for several non-odd nonlinearities f. In our theorems we do not assume oddness, and so it was gratifying to see that the algorithms still converged to the expected solutions.

5 Existence of Solutions.

The proofs in this section hold for a more general class of nonlinearity than those typically used in our numerical experiments. We assume essentially the same hypothesis found in [1], [9], [21] and [4]. In particular, we take $f \in C^1(\mathbb{R}, \mathbb{R})$ such that $f(0) = 0$ and the following conditions hold. Our key assumption is that f is *superlinear*, i.e.,

$$\lim_{|u|\to\infty} \frac{f(u)}{u} = \infty. \tag{15}$$

We also make use of the convexity assumption

$$f'(u) > \frac{f(u)}{u} \quad \text{for } u \neq 0. \tag{16}$$

We assume that $f'(0) < \lambda_1 = 0$, although as in [7] it is almost assured that one could relax this condition to $f'(0) < \lambda_2$ and still obtain sign-changing solutions (the proofs in that paper deal with technical difficulties due to the lack of compactness and infinite dimensionality that are not likely to arise here).

In the continuous case (2) one must make additional assumptions. For completeness we include them here. In [4], we additionally assume that there exists $m \in (0,1)$ such that

$$\frac{m}{2} f(u)u \geq F(u) \tag{17}$$

(in fact this need only hold for $|u| > \rho$ for some $\rho > 0$). This condition implies the coercivity of J on S and is used to make up for the loss of compactness when proving convergence of minimizing sequences. Analysis of the PDE also requires that we assume that there exist constants $A > 0$ and $p \in (1, \frac{N+2}{N-2})$ such that $|f'(u)| \leq A(|u|^{p-1}+1)$ for all $u \in \mathbf{R}$. It follows that f is *subcritical*, i.e., there exists $B > 0$ such that $|f(u)| \leq B(|u|^p + 1)$. For $N = 1$ this condition is omitted, while for $N = 2$ it suffices to have $p \in (1, \infty)$ (see [1]). In our finite dimensional setting the coercive and subcritical assumptions appear unnecessary, but might come in handy if one attempted to get a "convergence result", i.e., look at a family of graphs increasing in order and try to say something about a continuous problem that was being approximated.

We are not concerned with loss of compactness, subcritical growth, or the Sobolev Embedding Theorem in our finite dimensional setting. Clearly our functional J is well defined and twice differentiable on all of $\mathbb{R}^m$.

We first present a Lemma, which represents something of an obstacle towards applying the techniques from [4]. We note that in the continuous case, the equivalent equation is $\int_\Omega \nabla u_+ \cdot \nabla u_- \, dx = 0$, which implies the nice additivity properties $J(u) = J(u_+) + J(u_-)$, $J'(u)(u) = J'(u_+)(u_+) + J'(u_-)(u_-)$, and so on.

Lemma 5.1 *Given $u \in \mathbb{R}^m$ we have $Lu_+ \cdot u_- = Lu_- \cdot u_+ \geq 0$.*

Proof. Using the notation that k_x is the degree of vertex $x \in V$ and that $x_i,\ i = 1, \cdots, x_k$ are the neighbors of x, we see that

$$Lu_+ \cdot u_- = \sum_{x \in V} \{k_x u_+(x) - \sum_{i=1}^{k_x} u_+(x_i)\} u_-(x) \geq 0, \tag{18}$$

since the only possible nonzero terms are the result of positive neighbors $u_+(x_i)$ multiplying the negative value $u_-(x)$. ∎

We now state some of the useful properties of the Nehari manifold S defined in (6) and of the functional J acting on or near S. We take $\lambda < \lambda_1 = 0$; otherwise, S is degenerate and fails to be a manifold.

1. S is a closed $m-1$ dimensional C^1 manifold in $\mathbb{R}^m$.
2. $J''(0)(u,u) > 0$ for all $u \in \mathbb{R}^m$, $0 \notin S$, and $J \geq c > 0$ on S.
3. S is bounded (unlike the infinite dimensional case).
4. J is bounded above on S (unlike the infinite dimensional case).
5. Given $u \neq 0 \in \mathbb{R}^m$ there exists unique $\alpha > 0$ so that $\alpha u \in S$.
6. For $u \in S$, $J(u) > J(tu)$ for all $t \in [0,\infty) - \{1\}$ and $J''(u)(u,u) < 0$.
7. u is a nontrivial solution to (1) if and only if u is a critical point of $J|_S$.

These facts follow from arguments which are virtually identical to those found in [4]. The fact that S is closed (0 is not a limit point of S) was claimed in [4] and later proven in [17]. In this finite dimensional setting, this is obvious. That S is a manifold follows from the Implicit Function Theorem. Observe that S is the zero-set of $\gamma(u) = J'(u)(u) = Lu \cdot u - u \cdot f(u)$. Then by (16) and for $u \in S$ we have

$$J''(u)(u,u) = Lu \cdot u - u^2 \cdot f'(u) < Lu \cdot u - u \cdot f(u) = \gamma(u) = 0. \qquad (19)$$

That is to say, the gradient of γ is non vanishing on its zero set, which is thus a manifold. Note that

$$J''(0)(u,u) = Lu \cdot u - f'(0)u \cdot u > 0$$

by the Poincare inequality (or characterization of the smallest eigenvalue $\lambda_1 = 0$). Since 0 is a local minimum and f superlinear implies that for $u \not\equiv 0$ we have $J(\alpha u) \to -\infty$ as $\alpha \to \infty$, we see there must exist an $\alpha > 0$ so that $\alpha u \in S$. This α is unique, since (19) says every critical value in the ray direction must be a maxima. By Lagrange multipliers, u is a nontrivial critical point of J if and only if it is a critical point of $J|_S$. Indeed, if u is a constrained critical point then $\nabla J(u) = t\nabla\gamma(u)$ for some multiple t of the normal vector to S, $\nabla\gamma(u)$. This implies that $t = 0$ hence $\nabla J(u) = 0$, since (19) gives $\gamma(u) \cdot u < 0$ yet $\nabla J(u) \cdot u = 0$ (by virtue of $u \in S$). Since S is closed and bounded hence compact (due to the finite dimension of $\mathbb{R}^m$), the continuous function J must be bounded on S. In this discrete case it is not hard to see that there exists $\delta > 0$ so that $J(u) \geq \delta > 0$ for all $u \in S$. Some of these facts are less useful than in the continuous case, since we are now

dealing with a compact manifold and do not, for example, have to worry if bounded sequences have only weakly convergent subsequences.

We now prove **Theorem 2.1**:
Proof. Let $\{u_n\} \subset S$ be a minimizing sequence, i.e., $J(u_n) \downarrow \min_S J$. Since S is a compact set, there exists a subsequential limit $u \in S$ satisfying $J(u) = \min_S J$. By the above discussions, the constrained mininima is in fact a critical point of J, hence a solution to (1). Suppose that u was sign-changing. Since u is a solution and hence $J'(u)(u_\pm) = 0$, Lemma 5.1 implies that $\gamma(u_\pm) \leq 0$. Without loss of generality, let $0 < c \leq d \leq 1$ be such that $cu_+, du_- \in S$. Then

$$J(u) \geq J(cu) \geq J(cu_+) + J(cu_-) > J(cu_+),$$

since $\gamma(du_-) = 0$ and $c \leq d$ implies that $J(cu_-) > 0$. This is a contradiction, since $cu_+ \in S$ yet $J(u) = \min_S J$. Thus, u is a one-sign solution to (1). If f is odd, $-u$ is automatically a critical point of the even functional J, hence a one-sign solution of the opposite sign. Suppose that f is not odd and without loss of generality assume that the solution we just found was positive. Then, we can repeat the above argument using $\tilde{f}$ defined by $\tilde{f}(u) = -f(-u)$ for $u > 0$ and $\tilde{f}(u) = f(u)$ for $u \leq 0$ to get a pair of one-sign solution. Since we are using the other branch of f, the negative solution is in fact a negative solution to the original problem. ∎

The proof of **Theorem 2.2** is almost a corollary:
Proof. Let $\{u_n\} \subset S$ be a maximizing sequence, i.e., $J(u_n) \uparrow \max_S J$. Since S is a compact set, there exists a subsequential limit $u \in S$ satisfying $J(u) = \max_S J$. By the above discussions, the constrained mininima is in fact a critical point of J, hence a solution to (1). ∎

If nondegenerate, the minimizers are MI 1 and the maximizer is of MI m. It seems almost assured that the maximizer is a sign-changing solution, but we have not proven this. One need only show that given $u \in S$ of one-sign that there exists $v \in S_1$ with $J(u) < J(v)$ to confirm this conjecture, which seems likely when viewing Figure 6.

We now prove **Theorem 2.3**:
Proof. As in [4], the separation property of S_1 is key. Accordingly, let $u \in S_1$ and consider $z(t) = P_S((1-t)u_+ + tu_-) = \alpha(t)((1-t)u_+ + tu_-)$,

for some smooth function $\alpha : [0,1] \to (0,2]$. Clearly $\alpha(\frac{1}{2}) = 2$, so that $z(\frac{1}{2}) = u \in S_1$. Now suppose that $\frac{d}{dt}(J(z(t))) = 0$ for some $t = t^*$. Since $z \in S$, $0 = J'(z)(z) = J'(z)(z_+) + J'(z)(z_-)$ so that $J'(z)(u_-) = \frac{t-1}{t} J'(z)(u_+)$. Since

$$0 = \frac{d}{dt}(J(z(t))) = \frac{\alpha'}{\alpha} J'(z)(z) + \alpha J'(z)(u_- - u_+) = \alpha J'(z)(u_- - u_+),$$

we have

$$J'(z)(u_-) = J'(z)(u_+) = \frac{t-1}{t} J'(z)(u_+).$$

This implies that $J'(z)(u_-) = J'(z)(u_+) = 0$, hence $\gamma(z_\pm) \leq 0$, since $\frac{t-1}{t} \neq 1$. By (16),

$$J''(z_\pm)(z_\pm, z_\pm) = Lz_\pm \cdot z_\pm - z_\pm^2 \cdot f'(z_\pm) < Lz_\pm \cdot z_\pm - z_\pm \cdot f(z_\pm) = \gamma(z_\pm) \leq 0.$$

Now, using Lemma (5.1) we obtain

$$\begin{aligned}
\tfrac{d^2}{dt^2}(J(z(t))) &= \alpha' J'(z)(u_- - u_+) + \alpha^2 J''(z)(u_- - u_+, u_- - u_+) \\
&= \alpha^2 j''(z)(u_- - u_+, u_- - u_+) \\
&= \tfrac{1}{t^2} J''(z_+)(z_+, z_+) + \tfrac{1}{(1-t)^2} J''(z_-)(z_-, z_-) - 2\alpha^2 L u_+ \cdot u_- \\
&< 0.
\end{aligned}$$

Hence, the critical point of $J \circ z$ for $t \in (0,1)$ is unique and a maximum, For this value t^*, we have $J(z)(z_- - z_+) = 0$ and so $u = z(t^*) \in S_1$ and $J(u) > J(z(t))$ for all $t \in [0,1] - \{\frac{1}{2}\}$. In fact, S_1 separates any $v > 0$ and $w < 0$ on S. Let $z : [0,1] \to S$ now denote any path on S so that $z(0) = v$ and $z(1) = w$. For $0 < t << \frac{1}{2}$, one sees that $\gamma(z) = 0$, $\gamma(z_-) > 0$, and $\gamma(z_+) < 0$ (see Figure 1). Similarly, for $1 > t >> \frac{1}{2}$, we have that $\gamma(z) = 0$, $\gamma(z_-) < 0$, and $\gamma(z_+) > 0$, implying that

$$J'(z)(z_- - z_+) = \gamma(z_-) - \gamma(z_+)$$

changes sign for some $t = t^* \in (0,1)$. For $u = z(t^*)$ we have that $J'(u)(u_- - u_+) = 0$ hence $u \in S_1$.

Proceeding as in the one-sign existence proof, we find a minimizer $u \in S_1$ satisfying $J(u) \geq J(v)$ for all $v \in S_1$. We do not know that S_1 is a manifold

and so cannot apply Lagrange multipliers. However, if we suppose that u is not a solution we can find a contradiction. As in [4], take the path $z(t) = P_S((1-t)u_+ - tu_-)$ and in a neighborhood about u apply the Deformation Lemma. As a result, we would follow the negative gradient flow (projected tangent to S, we know the a nonzero gradient cannot be orthogonal to S) and obtain a deformed path which a) still connects positive to negative elements of S and hence intersects S_1 by the above separation property, and b), has a strictly smaller maximum J value along it. This cannot be, since we started the flow with a path through the minimizer of $J|_{S_1}$. Thus, we have a solution which necessarily changes sign by virtue of membership in S_1. An argument very similar to the one-sign case shows that the solution must change sign exactly once. If not, we could construct an element of S_1 with strictly smaller J value, another contradiction. ∎

We conclude with the proofs of **Theorem 2.4** and **Theorem 2.5**:
Proof. If $\{u_n\}$ is a minimizing (maximizing) sequence in $S \cap \chi$, then as above we get a subsequential limit. The resulting minimizer (maximizer) u is in $S \cap \chi$. By Lagrange multipliers, we know that $\nabla J(u)$ cannot be nonzero and normal to S. By invariance, the gradient lies in χ. Thus, the constrained critical point of $J|_{S\cap\chi}$ is a critical point of J and hence a solution to (1) with the symmetry type corresponding to the fixed point subspace χ.

Let χ be a fixed point subspace with the property that if $u \in \chi$ with $u_+, u_- \neq 0$ then also $u_+, u_- \in \chi$. If $\{u_n\}$ is a minimizing sequence in $S_1 \cap \chi$, then as above we get a subsequential limit. The resulting minimizer u is in $S_1 \cap \chi$. Now, the path $z(t) = P_S((1-t)u_+ + tu_-) \in S \cap \chi$ as well, since $u_+, u_- \in \chi$. Again using the invariance of the gradient, we see that assuming that $\nabla J(u) \neq 0$ leads to a contradiction. This follows from the fact that the deformed path will also lie in χ, so that the separation property of S_1 yields an element of $S_1 \cap \chi$ with strictly lower J value than the minimum value $J(u)$. Necessarily, this solution changes sign and is of a symmetry type corresponding to the fixed point subspace.

Finally, let χ be a fixed point subspace with the property that if $u \in \chi$ then $u_+, u_- \neq 0$. Using above arguments, we get a convergent minimizing sequence of $J|_{S\cap\chi}$. Using the symmetry invariance of the gradient, we see that the minimizer is a solution without the need to appeal to the deformation lemma. This follows since $S \cap \chi$ is a manifold. In hindsight, this solution belongs to S_1 since it is a solution which changes sign. It is of a symmetry type corresponding to the fixed point subspace.

∎

All of the above proofs can be seen in action by studying the simple example $G = \mathbf{K}_3$ in Section 4. For example, consider the sign-changing symmetry type B branch corresponding to ψ_3. Any sign changing vector u of the form (b, b, a) (without loss of generality assume that $b < 0$) has $u_+ = (0, 0, a)$ and $u_- = (b, b, 0)$ of type B as well. Thus, the paths on S connecting $\alpha u_+ \in S$ to $\alpha u_- \in S$ (which must pass through S_1) are composed of elements also of type B. Minimization in $S_1 \cap \chi_B$ necessarily results in a sign-changing solution of symmetry type B. Additionally, consider the type D branch which also bifurcates from $\lambda_2 = \lambda_3 = 3$. It is not true that elements of this symmetry type have positive and negative parts of the same symmetry type, but by virture of the the symmetry type, such elements are already sign-changing if nontrivial. Thus, minimization in $S \cap \chi_D$ results in a sign-changing solution of symmetry type D. In both cases for this low-dimensional example we in fact obtained isolated points when intersecting an invariant subspace with either S or S_1. Thus, minimizing sequences are constant in $\chi_B \cap S_1 \neq \emptyset$ and $\chi_D \cap S \neq \emptyset$, since $\dim(\chi_B \cap S_1) = 0$ and $\dim(\chi_D \cap S) = 0$.

As a final comment, there is much that could be proven concerning bifurcation. Our automated code in [19] relies on developed theory of symmetry, fixed point subspaces, and bifurcation (see for example [12]). The Equivariant Branching Lemma (EBL) is perhaps the core tool we use to predict bifurcation. It is useful to ponder when writing code to find new bifurcation branches, and should prove equally useful in proving theorems concerning the existence of such branches. The EBL implies the "bifurcation from simple eigenvalues" results used so heavily by nonlinear functional analysts studying variational functionals for elliptic PDE (see for example [21]).

6 Conclusion.

Thus, we have developed a new field of study, partial difference equations (PdE) on graphs. Open questions and areas for future inquiry abound. Extending the representation theory found in [18] to analyze symmetry types of eigenvectors for the discrete Laplacian is an obvious first step. Not only is this of interest in its on right, but it is an essential step towards understanding all possible solutions to nonlinear elliptic equations. It is not clear that there

exists in all cases a "cannonical" basis; perhaps orthogonality and symmetry types do not always go hand in hand. Calculating the conjugacy classes of the symmetry group as done here and in [19] for larger graphs with varying degrees of symmetry is the next step, as this will enable the implementation of automated branch following where decisions based on symmetry aid in following bifurcating branches at multiply degenerate bifurcation points. In future efforts, we may use the code recently developed by the author's colleague N. Sieben using GAP (Graphs, Algorithms, and Programming, see `http://www.gap-system.org/gap/`) to automate the process of cataloging symmetry types and ordering the basis. For large graphs, the ARPACK code of [18] or perhaps the parallel version PARPACK will be necessary in order to efficiently compute the eigenpairs. We are interested in embedding graphs in to metric spaces, whereby one might be able to approximate PDE on manifolds using ideas from this paper. Weighted Laplacians could be used. This might be interesting in itself, or, if the weights are chosen depending on the location of vertices in a metric space, then again approximations to PDE might be obtained. It may be necessary to use Monte Carlo integration methods to form the gradients and Hessians when investigating elliptic PDE on high-dimensional regions. This suggests that perhaps the same random distribution of points could define a random graph, and the corresponding (weighted?) Laplacian might be used to generate a matching basis.

Graphs of all types of symmetry abound; it has been suggested that the Peterson graph and the Gray semi-symmetric (bipartite) graph will be interesting. We ran experiments on non symmetric (and much less symmetric) graphs analogous to the small complete graphs experiments detailed above. In particular, we wondered if a small graph with simple eigenvalues would be free of secondary bifurcations. The answer is "not necessarily"; we found secondary bifurcations when investigating a non symmetric graph with 5 vertices. A systematic approach is likely to be fruitful, although perhaps no more (or less) conclusive than the typical foray in to questions of classification in graph theory.

The GNGA amounts to a simple application of Newton's method on $K : \mathbb{R}^m \to \mathbb{R}^m$ defined by $Ku = -Lu + f(u)$, but uses the symmetry of the graph and solutions of an associated linear problem to sufficiently understand the basins of attraction. Clearly the large amount of known theory (over 100 papers) related to graphs and their Laplacians will be useful in the future research of nonlinear PdE.

One could consider types of PdE other than elliptic. Any PDE with

a '$-\Delta$' in it could be converted to a PdE using Laplacians on graphs, in fact, derivatives of any order can be replaced with an appropriate difference matrix. As a first forray in to these other areas, we considered the following parabolic and hyperbolic equations:

$$\begin{cases} u_t &= -Lu \\ u(0) &= u_0 = \sum_{i=1}^m a_i\psi_i \\ & \\ & \text{and} \\ & \\ u_{tt} &= -Lu \\ u(0) &= u_0 = \sum_{i=1}^m a_i\psi_i \\ u'(0) &= v_0 = \sum_{i=2}^m b_i\psi_i \ (v_0 \cdot \mathbf{1} = 0 \implies b_1 = 0), \end{cases}$$

where one seeks solutions $u : (0, \infty) \to \mathbb{R}^m$, again identifying $\mathbb{R}^m$ with functions mapping V to $\mathbb{R}$. These elementary first and second order linear systems can be solved in a straightforward way using separation of variables. Respectively, the solutions can be written as

$$\begin{cases} u(t) &= \sum_{i=1}^m a_i e^{-\lambda_i t}\psi_i = (e^{-tL})u_0 \\ & \\ & \text{and} \\ & \\ u(t) &= \sum_{i=1}^m a_i \cos(\lambda_i^{\frac{1}{2}}t)\psi_i + \sum_{i=2}^m (b_i/\lambda_i^{\frac{1}{2}}) \sin(\lambda_i^{\frac{1}{2}}t)\psi_i \\ &= \cos(tL^{\frac{1}{2}})u_0 + L^{\dagger\frac{1}{2}} \sin(tL^{\frac{1}{2}})v_0, \end{cases}$$

where $\dagger$ denotes a pseudo inverse. Numerical experiments using explicit and implicit methods generated satisfactory approximations to the above solutions. Considering the extension of these non-elliptic equations to nonlinear situations, equations of mixed typed, the inclusion of other order difference terms, and complicated graphs obviously leads to a field of study nearly as large as that of all of PDE.

The author thanks Nandor Sieben, Jim Swift, and Steve Wilson of Northern Arizona University for their help in suggesting graphs and explaining the associated symmetries. The articles [18] and [19] contain a much more detailed explanation of the symmetry arguments found in Figure 3.

References

[1] A. Ambrosetti and P. Rabinowitz, *Dual Variational Methods in Critical Point Theory and Applications*, J. Functional Analysis **14** (1973), pp. 349-381.

[2] R. B. Bapat, *The Laplacian Matrix of a Graph*, Math. Student **65** (1996), no. 1-4, pp. 214-223.

[3] N. Biggs, *Algebraic Graph Theory. Second edition.*, Cambridge Mathematical Library. Cambridge University Press, Cambridge, 1993. viii+205 pp.

[4] A. Castro, J. Cossio and John M. Neuberger, *A Sign-Changing Solution for a Superlinear Dirichlet Problem*, Rocky Mountain J. of Math., **27**, No. 4 (1997), pp. 1041-1053.

[5] A. Castro, J. Cossio and John M. Neuberger, *On Multiple Solutions of a Nonlinear Dirichlet Problem*, Nonlinear Analysis TMA, **30**, No. 6 (1997), pp. 3657-3662.

[6] A. Castro, J. Cossio and John M. Neuberger *A Minimax Principle, Index of the Critical Point, and Existence of Sign-Changing Solutions to Elliptic Boundary Value Problems*, Electronic J. of Diff. Eq., Vol. 1998 (1998), No. 2, pp. 1-18.

[7] A. Castro, P. Drabek and John M. Neuberger, *A Sign-Changing Solution for a Superlinear Dirichlet Problem, II*, Proceedings of the Fifth Mississippi State Conference on Differential Equations and Computational Simulations (Mississippi State, MS, 2001), 101–107 (electronic), Electron. J. Differ. Equ. Conf., 10.

[8] D. Costa, Z. Ding, and John M. Neuberger, *A Numerical Investigation of Sign-Changing Solutions to Superlinear Elliptic Equations on Symmetric Domains*, J. Comput. Appl. Math. **131** (2001), pp. 299-319.

[9] Y. S. Choi and P. J. McKenna, *A mountain pass method for the numerical solution of semilinear elliptic problems*, Nonlinear Anal. **20** (1993), no. 4, pp. 417-437.

[10] F. Chung, *Spectral graph theory*, CBMS Regional Conference Series in Mathematics, 92. Published for the Conference Board of the Mathematical Sciences, Washington, DC; by the American Mathematical Society, Providence, RI, 1997. xii+207 pp.

[11] J. Cossio, S. Lee, John M. Neuberger, *A Reduction Algorithm for Sublinear Dirichlet Problems*, Proceedings of the Third World Congress of Nonlinear Analysts, Part 5 (Catania, 2000). Nonlinear Anal. **47** (2001), no. 5, pp. 3379-3390.

[12] M. Golubitsky, I. Stewart, D. Schaeffer, *Singularities and groups in bifurcation theory. Vol. II*, Applied Mathematical Sciences, **69**. Springer-Verlag, New York, 1988. xvi+533 pp.

[13] L. Ljusternik and L. Schnirelmann, *Methodes Topologique dans les Problemes Variational*, Hermann and Cie, Paris (1934).

[14] John M. Neuberger and J. W. Swift, *Newton's Method and Morse index for Semilinear Elliptic PDEs*, Internat. J. Bifur. Chaos Appl. Sci. Engrg. **11** (2001), no. 3, pp. 801-820.

[15] John M. Neuberger, D. Rice, and J. W. Swift, *Numerical Solutions of a Vector Ginzburg-Landau Equation with a Triple Well Potential*, Int. J. Bif. and Chaos (To Appear Fall 2003).

[16] John M. Neuberger, *A numerical Method for Finding Sign-Changing Solutions of Superlinear Dirichlet Problems*, Nonlinear World **4** (1997), no. 1, pp. 73-83.

[17] John M. Neuberger, *A sign-changing solution for a superlinear Dirichlet problem with a reaction term nonzero at zero*, Nonlinear Anal. **33** (1998), no. 5, pp. 427-441.

[18] John M. Neuberger, N. Sieben, and J. W. Swift, *Computing Eigenfunctions on Koch's Snowflake: A New Grid and Symmetry*, Preprint, 2003.

[19] John M. Neuberger, N. Sieben, and J. W. Swift, *Semilinear BVP on Koch's Snowflake: Symmetry and Automated Branch Following using GNGA (Tentative Title)*, Preprint, 2003.

[20] J. W. Neuberger, *Sobolev gradients and differential equations*, Lecture Notes in Mathematics, **1670**. Springer-Verlag, Berlin, 1997. viii+150 pp.

[21] P. H. Rabinowitz, *Minimax methods in critical point theory with applications to differential equations*, CBMS Regional Conference Series in Mathematics, 65. Published for the Conference Board of the Mathematical Sciences, Washington, DC; by the American Mathematical Society, Providence, RI, 1986. viii+100 pp.